Robot Grasp Sunthesis Under Object Pose Uncertainty

Submitted: 4th November 2014; accepted: 8th January 2015

Wojciech Szynkiewicz

DOI: 10.14313/JAMRIS_4-2014/7

Abstract:

This paper addresses the problem of grasp synthesis for grasping objects considering both object pose uncertainty and object dynamics. These two factors greatly affect success or failure in a real-world robotic grasping and should be considered simultaneously. The proposed approach is based on simulation of grasping process assuming that the 3D model of the object is known. Object geometry is modelled using superquadrics. To evaluate grasp quality three different measures are utilised. The proposed grasp synthesis approach will be implemented and tested on a real robot with multi-fingered hand.

Keywords: *grasp synthesis, pose uncertainty, grasp quality*

1. Introduction

Grasping and manipulation of various objects are one of the fundamental features of rescue and exploration robots as well as service robots. In real-world scenarios, especially in unstructured environments, reliable and stable grasping of everyday objects with complex grippers, such as multi-fingered robotic hands is still a major challenge and important research problem [1, 3, 11, 12, 20, 21]. Successful grasping enables a robot to physically interact with the environment and accomplish other object manipulation tasks. This paper deals with the problem of grasp synthesis in the presence of uncertainty. We consider grasp planning for known objects assuming that the 3D geometric model of an object is available and there is uncertainty about the relative pose of the robot and the object.

Acquiring a grasp on an object requires grasp synthesis to determine proper contact points on the object surface and an appropriate gripper configuration. In order to synthesise a correct grasp the following characteristics should be taken into account: stability, disturbance resistance, dexterity, and task-compatibility. The most fundamental requirement of any grasping strategy is to guarantee grasp stability. A grasp is stable if any bounded deviation in the object pose caused by an external disturbance vanishes in time after this disturbance disappears. Typically disturbances arise from inertial forces or externally applied forces such as those due to gravity. Stability is a necessary but not a sufficient condition for obtaining a successful grasp. Besides stability, it is usually required the grasp to be compatible with the task requirements. A grasp should immobilize the object with respect to the gripper under all wrenches (forces and torques) expected during the task execution. The grasps that can be maintained for every possible disturbance are known in the literature as closure grasps. The two extensively used properties of grasp restraint are *force closure* and *form closure* [16,20]. The grasp is form-closure, if the location of the contacts makes any motion of the object with respect to the gripper impossible, regardless of external wrench magnitude. Obviously, preventing all motion is possible only if contacting bodies are rigid. In other words, the object is form closed when the palm and fingers enclose the object and fully constrain it. This property is used when a robust grasp, not relying on friction, is required to accomplish the task. A grasp has force closure property when the fingers can apply, through the set of contact points, appropriate forces to ensure the object immobility. The grasp is force closed if it is capable of resisting any external wrench applied on the object and holding it in equilibrium. The force closure property is utilised when dexterous manipulation of objects with a low number of frictional contacts is required.

Napier [17], in his study on the prehensile movements of the human hand, distinguished two primary grasping patterns, *power grasps* and *precision grasps*. Power grasps are characterized by large contact areas between the object and the hand. Thus, this type is chosen when considerations of stability and security predominate. Typically, power grasps are used when we want to apply a large force to the object. An example of a power grasp is the squeeze grip of a hammer handle while driving in nails. The major characteristic of precision grasps is that the object is touched with the fingertips, and contact area is small. Precision grasps are used when high dexterity and manipulability of the grasped object is required. Writing with a pencil is a typical example of a precision grip. It should be noted that depending on the purpose of the grasp, the same object can be held with either of the two types of grasp.

Given an object, grasp synthesis pertains to the problem of finding a grasp configuration (specific pose for the hand, as well as configuration for the fingers) that satisfies a set of constraints. Generally, a good grasp should satisfy the three sets of constraints: hand constraints, object constraints, and task constraints.

A grasp can be formally defined as a set of contacts on the surface of the grasped object together with friction cone conditions [16]. Grasp synthesis is then usually formulated as a problem of finding contact locations in order to optimize a specific grasp

quality measure. The study of grasp synthesis can be classified into two broad groups: analytical methods and empirical methods [21, 22]. In the analytical approach grasping is modeled in terms of contact locations and forces, using the laws of physics. Grasp synthesis methods rely on mathematical models of the interaction between the object and the hand. If object properties such as shape, size, weight, material properties and pose are known, grasp synthesis using analytical approaches can be used. However, analytical methods are usually based on assumptions such as simplified contact models, Coulomb friction, and rigid body modeling [16,20]. Grasp planning is often formulated as a large scale, constrained non-linear optimization problem with an objective function according to a predefined grasp quality criterion [15]. Empirical or data-driven strategies for grasp synthesis can be divided into two main groups: (1) systems based on the observation of the object to be grasped and (2) systems based on the observation of a human performing the grasp [3]. Empirical approaches rely on sampling grasp candidates for an object and ranking them according to a specific measure or metric. In empirical approaches usually various classification and learning techniques are utilised. In contrast to analytical techniques, empirical methods pay more attention on the object representation and the sensory data processing, similarity metrics, object recognition, and shape and pose estimation.

Most of the traditional methods for precision grasp synthesis provide precise contact locations for the fingers on the object surface. To perform a correct grasp, a robot has to be able to precisely reach these contact locations and exert precise forces. In simulation and highly structured environments this can be viable, but when grasping objects with a real mechanical hand, inaccuracies and uncertainties, especially in the object shape and/or pose, restrain the robot from reaching these contact locations. In practice, spatial uncertainty is inherent to any grasping system and is due to perceptual and actuation errors, as well as modeling errors of the robot system and the object. These geometric uncertainties can directly influence the relative configuration between the hand and object, upon which the grasp stability is built. Only if execution is robust to uncertainties in sensing and actuation, a grasp can succeed with high probability. To cope with uncertainty in grasping by locally adjusting the hand pose or the finger joint angles sensory feedback is used [5, 6, 14].

Since we are using models of the objects, the uncertainty comes mainly from the location of the object. In our work, we employ a sampling based approach to consider pose uncertainty. We use a probabilistic distribution model for the pose error and incorporate object dynamics along with three metrics into the grasp quality evaluation. The goal is to develop grasp synthesis method that will be implemented on the two-handed robot Velma. The Velma robot is a two-arm manipulator with two Kuka LWR-4+ arms and two Barrett Hands (see Fig. 1). The robot has a variety of sensors for accomplishing perception tasks. The remainder of this paper is structured as follows. Section 2 refers to related work on grasp synthesis under pose uncertainty. Section 3 presents motivation for our research and describes models used in this work. In Section 4 the grasp synthesis method is presented. The final conclusions are drawn in Section 5.

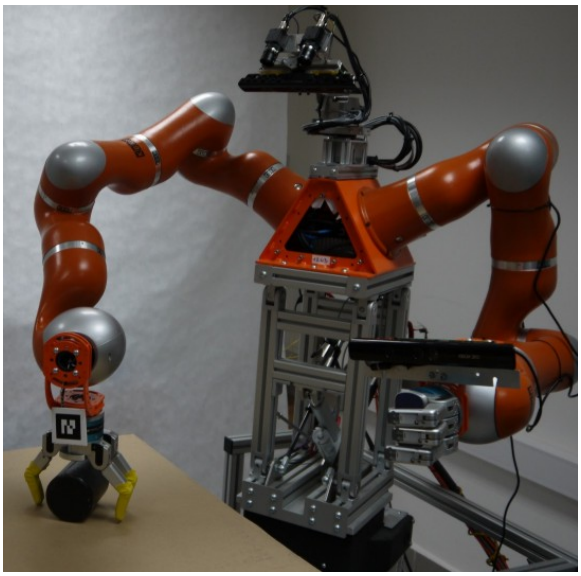

Fig. 1. Two-arm robot Velma

2. Related Work

There has been some previous work on grasp planning under uncertainty [4–6,12,14,25]. Uncertainty in robot grasping is commonly approached by more or less traditional statistical methods. In one of the earliest works dealing with grasp uncertainty [4], Brost proposed a method to grasp a polygonal planar object with a parallel-jaw gripper, when the object pose is not known precisely. A sequence of squeezing operations is planned in order to increasingly reduce the possible uncertainty on the object location.

Weisz and Allen [25] have integrated pose uncertainty into the static grasp quality analysis by computing the probability of force-closure in the presence of pose error. They proposed a new quality metric to measure the robustness of a grasp under object pose uncertainty. Pose error is sampled uniformly from a 3D error model representing an object on a support plane and the existing force-closure analysis to compute the probability is applied. In [1] the authors derived a novel grasp measure for robust grasping from observations of human guided grasping. They proposed a method that involves a human interacting physically with a robot arm and hand, moving and guiding the robot into the grasping pose. The authors found that humans optimize a skewness metric, i.e., the divergence of alignment between hand and principal object axes. Kim et al. considered object dynamics and pose uncertainty on the performance in estimating the actual grasp success rates of a grasp in the real environment [12]. They observed that considering both object dynamics and pose uncertainty in

grasp synthesis enabled generation of more stable and natural grasp sets compared with a commonly used approach based on kinematic simulation and force closure analysis.

Recently, Dang and Allen in [6] proposed a tactile experience based grasping pipeline which utilizes tactile feedback to adjust hand posture during the grasping task of known objects and improves the performance of robotic grasping under pose uncertainty. Grasping is much more difficult when the geometry of objects in the environment is previously unknown. This can be further complicated by sensor noise, partial visibility, etc. Therefore, a representation of the shape uncertainty and a method for finding stable grasps with respect to this uncertainty is necessary for reliable grasp execution. One of the most used representations is Gaussian Process Implicit Surfaces (GPIS), a stochastic method to compute a continuous estimate of the object surface from sparse and noisy sensor data, with uncertainty [26].

Several works have studied the effects of shape uncertainty on grasp quality. Christopoulos et al. [5] sampled spline fits for 2D planar objects to measure the quality of potential grasps under shape uncertainty and used this to rank a set of randomly generated grasps. Laaksonen et al. [14] used Gaussian Processes to model distributions on grasp stability online from tactile measurements, and selected grasps using Markov Chain Monte Carlo sampling. Hsiao et al. [10] have introduced a method considering uncertainty in object shape and pose data by combining the data from a set of object detection algorithms using a probabilistic framework to find an optimal grasp. They used tactile sensing data to estimate hand-object relative pose for synthesizing the next hand trajectory so that a specific grasp can be achieved.

3. Problem Formulation

The amount of computation required to find a grasp for known objects depends, to a large degree, on the shape of the object and 3D model used to represent the object. There is a number of geometric representations used in grasp synthesis to model objects. Among them are raw 3D point clouds, 3D polygonal meshes, simple geometrical primitives, 3D CAD-like models, complex probabilistic models.

3.1. Object Modelling

One of the practical representations used to model various geometric shapes are superquadrics. Superquadrics are a family of parametric shapes that include superellipsoids, supertoroids, and superhyperboloids [2]. The most popular superquadrics, especially in computer vision and in computer graphics, are superellipsoids which are useful for a volumetric part-based object representation, because they are compact in shape and have a closed surface. A superellipsoid surface which is centered in the origin of the model coordinate frame, and has its axes aligned with x, y, z axes of the coordinate frame, has the following parametric representation in terms of surface parameters v, u [2]:

$$\boldsymbol{x}(v,u) = \begin{pmatrix} a_1 \ \cos^{\beta_1}(v) \ \cos^{\beta_2}(u) \\ a_2 \ \cos^{\beta_1}(v) \ \sin^{\beta_2}(u) \\ a_3 \ \sin^{\beta_1}(v) \end{pmatrix} \tag{1}$$

for $-\frac{\pi}{2} \leqslant v \leqslant \frac{\pi}{2}$ and $-\pi \leqslant u \leqslant \pi$, where $\boldsymbol{x} \in \mathcal{X} \subseteq \mathbb{R}^3$. a_1, a_2, and a_3 define the superquadrics dimensions along X, Y, Z axes respectively, while the exponents β_1, and β_2 determine the shape curvatures that define a smoothly changing family of shapes from rounded to square. Superquadrics are versatile models, that can be used to describe a wide range of simple shapes and solids, including spheres, ellipsoids, cylinders, cones, cuboids, etc. Superquadric parameters have an intuitive meaning and allow modelling of natural shapes with rounded corners and edges, as well as standard geometric solids with sharp corners and edges. Choosing appropriate values of β_1, β_2 various shapes can be produced, e.g. cuboids are produced when $\beta_1 \approx 0, \beta_2 \approx 0$, cylinders are produced when $\beta_1 = 1, \beta_2 \approx 0$, or ellipsoids are formed when $\beta_1 = 1, \beta_2 = 1$. Modelling capabilities of superquadrics can be enhanced by deforming them in different ways. In order to increase the flexibility of the model (1), several deformations can be applied such as tapering, bending, making cavities, etc. [2].

Superquadrics can be also used in the 3D shape reconstruction from point clouds produced by RGB-D sensors like Microsoft's Kinect and a time-of-flight camera or 3D laser scanners [23]. Humans are able to identify complex objects by separating them into parts. These parts are composed of different primitive shapes such as spheres, cylinders, boxes, etc., that can be assembled in various ways to create countless objects. Complete object model is obtained by sectioning a 3D object model into its significant parts and by describing the shape of each part. We use superquadrics for objects part identification, for their ability to describe a large variety of solids with only few parameters. For grasp synthesis such a representation is more informative than, for example, a polygonal mesh, because it is much easier to determine how to grasp an object that is represented as a combination of primitive shapes. Therefore, we use a union of superquadrics to represent known objects in an unified manner.

The implicit superquadric equation can be derived from the explicit form of (1):

$$\left(\left(\frac{x}{a_1} \right)^{\frac{2}{\beta_2}} + \left(\frac{y}{a_2} \right)^{\frac{2}{\beta_2}} \right)^{\frac{\beta_2}{\beta_1}} + \left(\frac{z}{a_3} \right)^{\frac{2}{\beta_1}} = 1 \tag{2}$$

All points $\boldsymbol{p} \in \mathbb{R}^3$ with coordinates (x, y, z) satisfying this equation lie on the surface of the model. Left side of the equation (2) is so called *inside-outside* function $F(\boldsymbol{p})$:

$$F(\boldsymbol{p}) = \left(\left(\frac{x}{a_1} \right)^{\frac{2}{\beta_2}} + \left(\frac{y}{a_2} \right)^{\frac{2}{\beta_2}} \right)^{\frac{\beta_2}{\beta_1}} + \left(\frac{z}{a_3} \right)^{\frac{2}{\beta_1}} \tag{3}$$

If $F(\boldsymbol{p}) = 1$ point $\boldsymbol{p}$ lies on the surface of the superquadric. If $F(\boldsymbol{p}) < 1$ the point lies inside, and if $F(\boldsymbol{p}) > 1$ it lies outside the surface of the model. This function is an example of implicit surface. The inside-outside function $F(\boldsymbol{p})$ can be used in simulation for efficient collision checking between the object and the hand. Based on shape information objects can be assigned to specific classes, and then suitable heuristics can be used to speed up the search for appropriate grasps. To represent an object as superquadrics in a global coordinate frame we have another parameters to express the translation $\boldsymbol{p} = [p_x, p_y, p_z]^T$ and orientation $q = \cos\frac{\theta}{2} + \sin\frac{\theta}{2}\hat{\boldsymbol{u}}$ (expressed as a unit quaternion q, which represents a rotation about the axis of rotation $\hat{\boldsymbol{u}}$ through an angle θ).

3.2. Model of Pose Uncertainty

Successful grasping requires the robotic hand to achieve accurate placement with respect to a target object. In practice, there is always uncertainty about the object pose even for known objects. To estimate the pose of an object, a visual sensor is typically used [13]. However, the error in the object pose estimation is inevitable, because the accuracy of vision systems is limited, e.g., due to imperfect calibration, and occlusions, especially when important features of the object are partially occluded. Even small errors in object pose may cause failures in grasping, such as dropping or result in different contacts from the originally planned grasp. Most existing tools for automatic grasp planning use kinematic simulation of the grasping process and grasp selection is based on a static analysis. The contact points are generated under the assumption that the object remains at the same place. In most cases, the object may move unexpectedly due to finger contacts during grasping. In consequence, the object pose and contact locations may change significantly when the fingers touch the object during grasping, as shown in Fig. 2. Thus, it is reasonable to attempt using a dynamic simulation technique, instead of the kinematic one, to predict the result of grasping more accurately. In such a case, a stable grasp obtained under the assumption that the object is stationary might be unstable, and vice versa. To simplify our considerations, we assume that the object is placed on a planar surface and restricted to a set of stable poses on this surface as shown in Fig. 3. Object pose estimate is an input data to grasp planning system, and it can be obtained from visual localization [13]. However, simultaneous estimation of translation and rotation poses a serious problem in many applications involving robotic perception. Dual quaternions (restricted to rotation and translation in the plane) can be used as a natural representation of uncertainty. Dual quaternion d_q can be written as [9]:

$$\bar{d}_q = q_1 + \varepsilon q_2,$$

where q_1 and q_2 are quaternions, and ε is characterized by its nilpotency property $\varepsilon^2 = 0$.

Rotation in the (x, y)–plane can be represented by the dual quaternion

$$\bar{d}_r = \left(\cos(\frac{\varphi}{2}) + 0\cdot i + 0\cdot j + \sin(\frac{\varphi}{2})\cdot k\right) + \varepsilon\cdot 0,$$

and a translation $(t_1; t_2)$ in the (x, y)–plane can be represented by the dual quaternion

$$\bar{d}_t = 1 + \frac{\varepsilon}{2}(0 + t_1\cdot i + t_2\cdot j + 0\cdot k),$$

where i, j, k are typical basis elements. Hence, a combination of rotation and translation (where the rotation is performed first) is given by

$$\begin{aligned}\bar{d}_t\cdot\bar{d}_r =& \left(\cos(\frac{\varphi}{2}) + \sin(\frac{\varphi}{2})\cdot k\right)\\ &+ \frac{\varepsilon}{2}\left[\left(\cos(\frac{\varphi}{2})t_1 + \sin(\frac{\varphi}{2}t_2)\right)\cdot i\right.\\ &\left.\left(-\sin(\frac{\varphi}{2})t_1 + \cos(\frac{\varphi}{2}t_2)\right)\cdot j\right]\\ =& d_1 + d_2 k + \varepsilon(d_3 j + d_4 k)\end{aligned}$$

Thus, we require only four values to represent rigid body motion on the plane:

$$\bar{d}_q = [d_1, d_2, d_3, d_4]^T,$$

where $\bar{d}_q$ is the dual quaternion.

It is easy to recover the original rotation angle and translation (assuming that the translation is performed after the rotation):

$$\varphi = \text{atan2}(d_2, d_1)$$

and

$$\begin{aligned}t_1 &= 2\,(d_1 d_3 - d_2 d_4)\\ t_2 &= 2\,(d_2 d_3 + d_1 d_4)\end{aligned}$$

A strategy proposed in [9] can be used to obtain a probability distribution for unit dual quaternions. Let $\mathbb{S}^1$ denote the unit circle in $\mathbb{R}^2$. A random vector $\bar{x} \in \mathbb{S}^1 \times \mathbb{R}^2$ is distributed according to the proposed distribution if its probability density function is given by

$$f(\bar{x}) = \frac{1}{N(\boldsymbol{C})}\exp(\bar{x}^T\boldsymbol{C}\bar{x}) \tag{4}$$

where $\boldsymbol{C}$ is a suitable symmetric parameter matrix and $N(\boldsymbol{C})$ a corresponding normalization constant. Now we can apply a typical Bayesian inference where $\bar{x}$ is an unknown system state and $\bar{z}$ is a noisy measurement of this state. The noise is represented by some random vector $\bar{v}$. This can be formulated using dual quaternion setting as

$$\bar{d}_z = \bar{d}_v\cdot\bar{d}_x \tag{5}$$

where $\bar{d}_v$ and $\bar{d}_x$ are distributed according to the distribution (4) with respective parameter matrices $\boldsymbol{C}_v$ and $\boldsymbol{C}_x$. Then, $\bar{d}_x$ given a fixed $\bar{d}_z$ is also distributed according to this proposed distribution. In this way, the combination of dual quaternions and the proposed

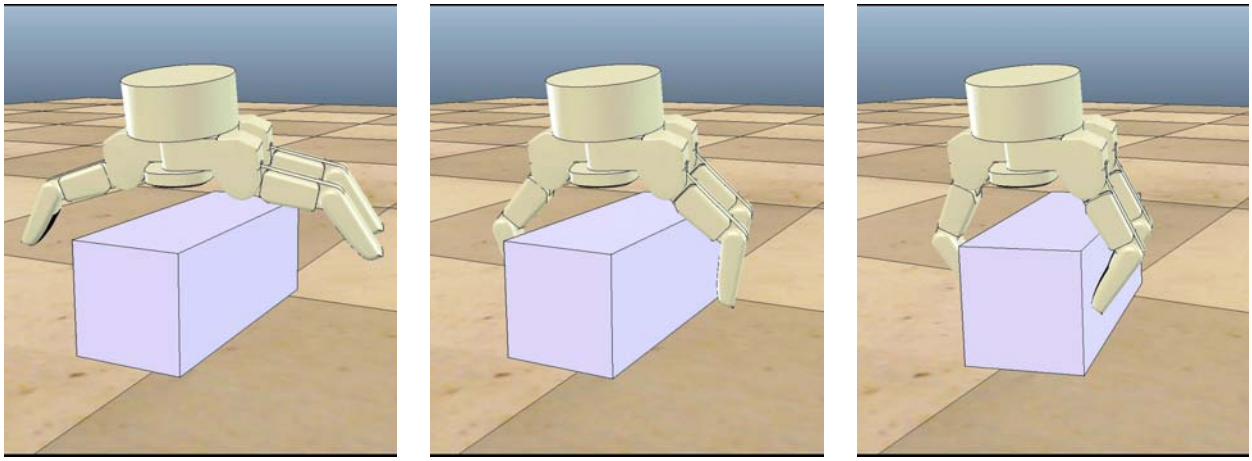

(a) (b) (c)

Fig. 2. Illustration of the effect of pose uncertainty during grasping

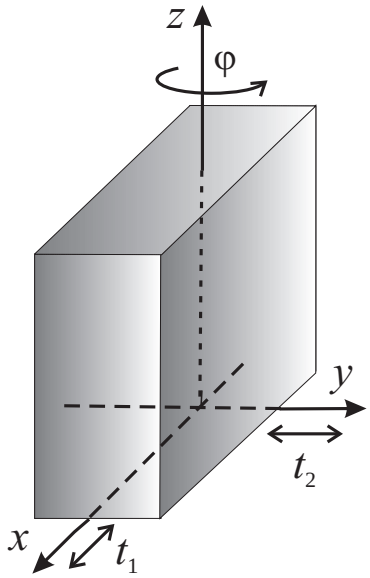

Fig. 3. Object pose uncertainty model in 2D space

probability distribution provides a closed form measurement update for simultaneous consideration of position and orientation.

One way to consider pose uncertainty is to run multiple grasping simulations starting from slightly different initial conditions for each grasp where the initial condition is set by sampling from an error model representing the pose uncertainty. To perform these simulations we use a 3D model (see Fig. 4) and kinematic model of the Velma robot running in the OpenRave simulation environment [7]. Object geometric and dynamics models are employed in the simulations. There are at least two reasons for employing a simulator for grasp synthesis and evaluation. Firstly, most real robot hand setups do not possess suitable sensors for evaluating the grasp quality needed to obtained good grasps. Secondly, to obtain a reliable grasp for every object in the face of pose uncertainty needs many grasp trials. It is not reasonable to perform this with a real robot hand.

3.3. Grasp Quality Measures

In order to compare different grasps on an object, metrics are needed. Depending on the task to be performed, different criteria can be evaluated. To evaluate the goodness of a grasp we use three quality measures. The first one, a modified $Q_1 = \varepsilon_{GWS}$ metric [8], that determines the magnitude of the largest worst-case disturbance wrench that can be resisted by a grasp. The second measure Q_2, which is called *skewness* [1], that measures the robot hand orientation relative to the object principal axis of inertia. Q_3 measure quantifies a deviation of the relative pose of the object to the hand from the initial relative pose [12]. These measures allow to assess different properties of the planned grasp. Q_1 measures disturbance resistance, and the magnitude of Q_1 yields a measurement which allows to rank grasps by their resistance to external disturbances. The second metric Q_2 measures hand orientation relative to the object principal axes of inertia and prefers grasps chosen by humans while grasping the same object, and finally, Q_3 indicates that a grasp is better if unintended object movement caused

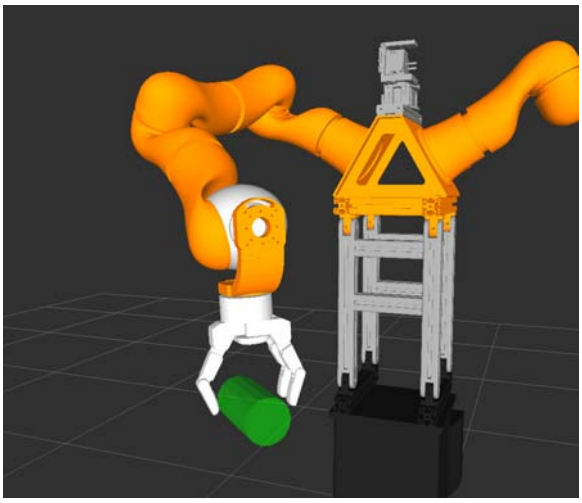

Fig. 4. 3D model of the Velma robot

by finger contacts is smaller.

Computing force closure grasps requires to compute the location of the contact points on the object surface and contact forces exerted in these points. Contact points $\boldsymbol{c}_i \in \mathbb{R}^3,\ i = 1, \ldots, k$ with corresponding inward pointing unit normal vectors $\boldsymbol{n}_i, \in \mathbb{S}_2 = \{\boldsymbol{n} \in \mathbb{R}^3 : \|\boldsymbol{n}\| = 1\}$. We assume that all contact forces are expressed in a reference frame O attached to the object, and its origin is located at the centroid of the contacts. A force $\boldsymbol{f}_i = \boldsymbol{f}_i^n + \boldsymbol{f}_i^s$ (where $\boldsymbol{f}_i^n$ is a normal component and $\boldsymbol{f}_i^s$ is a tangent component of the force vector) applied on the object at the point $\boldsymbol{c}_i$ generates a moment $\boldsymbol{m}_i = \boldsymbol{c}_i \times \boldsymbol{f}_i$ with respect to the reference point located at the origin of the object coordinate frame. The force and moment vectors are grouped in a wrench vector $\boldsymbol{w}_i = [\boldsymbol{f}_i^T, \lambda \boldsymbol{m}_i^T]^T \in \mathbb{R}^6$, with λ being a constant defined to introduce a metric on the wrench space.

A grasp wrench space (GWS) is characterized by the set of wrenches that can be applied to the target object from the contacts of a grasp, given certain limitations on applied forces. The grasp wrench space is bounded by the convex hull of the contact wrenches formed from the applied forces. The common constraint on the finger forces is that the sum of magnitudes of all the forces applied to the object is limited. Usually normalized limit of 1 is used, and the constraint is $\sum_i^k \boldsymbol{f}_i \leqslant 1$. If the contact forces obey the Coulomb friction model, then the space of all admissible contact forces forms a friction cone with opening angle $2\arctan(\mu)$, where μ is the coefficient of static friction. According to this model any contact force $\boldsymbol{f}_i$ that can be exerted without slippage at a point $\boldsymbol{c}_i$ with inward pointing normal $\boldsymbol{n}_i$ must lie in the friction cone $\mathcal{F}_i$, [8]:

$$\mathcal{F}_i = \left\{ \bar{\boldsymbol{f}}_i \ : \ \|\bar{\boldsymbol{f}}_i^s\| \leqslant \mu \, \|\bar{\boldsymbol{f}}_i^n\| \right\}, \tag{6}$$

where $\bar{\boldsymbol{f}}_i = \bar{\boldsymbol{f}}_i^n + \bar{\boldsymbol{f}}_i^s$. By approximating the friction cone at the contact point $\boldsymbol{c}_i$ by a pyramid with equally spaced m edges, the force $\bar{\boldsymbol{f}}_i$ can be expressed as a positive linear combination of forces $\bar{\boldsymbol{f}}_{i,j},\ j = 1, \ldots, m$ along the pyramid edges: $\bar{\boldsymbol{f}}_i \approx \sum_{j=1}^m \alpha_{i,j} \bar{\boldsymbol{f}}_{i,j}$, where $\sum_{j=1}^m \alpha_{i,j} = 1$ i $\alpha_{i,j} \geqslant 0$. The wrench $\boldsymbol{w}_i$ produced by $\bar{\boldsymbol{f}}_i$ at $\boldsymbol{c}_i$ can be expressed as a positive linear combination of the wrenches $\boldsymbol{w}_{i,j}$. The resultant wrench $\bar{\boldsymbol{w}}$ on the object is given by

$$\bar{\boldsymbol{w}} = \sum_{i=1}^{k} \bar{\boldsymbol{w}}_i = \sum_{i=1}^{k} \sum_{j=1}^{m} \alpha_{i,j} \bar{\boldsymbol{w}}_{i,j}, \tag{7}$$

By considering all possible variations of $\alpha_{i,j}$, the space $\mathcal{W}$ of possible resultant wrenches on the object is bounded by the convex hull of the union of primitive wrenches $\bar{\boldsymbol{w}}_{i,j}$, [8]:

$$\begin{aligned} \mathcal{CH}(\mathcal{W}) &= \mathcal{CH}\left(\bigcup_{i=1}^{k} \{\bar{\boldsymbol{w}}_{i,1}, \ldots, \bar{\boldsymbol{w}}_{i,m}\} \right) \\ &= \left\{ \sum_{i=1}^{k} \alpha_i \bar{\boldsymbol{w}}_i \,\middle|\, (\forall i : \alpha_i \geqslant 0) \ \wedge \ \sum_{i=1}^{k} \alpha_i = 1 \right\} \end{aligned} \tag{8}$$

In this case convex hull is a convex polyhedron.

Grasp quality measure Q_1 is defined as the largest perturbation wrench that the grasp can resist in any direction. It can be formulated as the minimum distance between the origin of the GWS and its boundary, which is defined as the convex hull of the union of primitive contact wrenches.

$$Q_1 = \varepsilon_{GWS} = \min_{\bar{\boldsymbol{w}} \in \mathcal{CH}(\mathcal{W})} \|\bar{\boldsymbol{w}}\|, \tag{9}$$

Geometrically, this quality measure is equivalent to the radius of the largest 6D ball centered at the origin of the wrench space and entirely contained in $\mathcal{CH}(\mathcal{W})$ if such a ball exists and zero otherwise. Force-closure is achieved when the origin of the wrench space lies strictly inside the $\mathcal{CH}(\mathcal{W})$.

The point on the convex hull closest to the origin of the GWS determines the "weakest" direction for the external disturbances. Figure 5a illustrates a 2D example of the grasp quality $Q_1 = \varepsilon_{GWS}$ where the GWS convex hull is spanned by 3 wrench vectors $\boldsymbol{w}_1, \boldsymbol{w}_2$ i $\boldsymbol{w}_3$. Efficient methods for computing ε_{GWS} quality metrics have been recently proposed [19, 27].

In order to increase the robustness to modelling errors we select only grasps with the quality value ε_{GWS} exceeding a given threshold ϱ, i.e. $\varepsilon_{GWS} > \varrho$. This threshold value should be determined experimentally, depending on the object properties and task to be performed.

The second criterion we are using to assess grasp quality is a measure based on the palm (or wrist) orientation relative to the main axis of inertia of the object [1]. In our case this quality index is adapted for the Barrett Hand. Let $\boldsymbol{v}$ be the unit vector perpendicular to the palm surface of the Barrett Hand, and $\boldsymbol{u}$ a vector along the object's principal axis of inertia as shown in Fig. 5b. The angle γ between both vectors may be computed as $\gamma = \arccos(\boldsymbol{u}^T \boldsymbol{v})$. Then, the skewness measure Q_2 is defined as

$$Q_2 = \begin{cases} \gamma & \text{if} \quad \gamma \leqslant \frac{\pi}{4} \\ \frac{\pi}{2} - \gamma & \text{if} \quad \frac{\pi}{4} < \gamma \leqslant \frac{\pi}{2} \\ \gamma - \frac{\pi}{2} & \text{if} \quad \frac{\pi}{2} < \gamma \leqslant \frac{3\pi}{4} \\ \pi - \gamma & \text{if} \quad \gamma > \frac{3\pi}{4} \end{cases} \tag{10}$$

We introduce the second criterion in order to select grasps that are distinguished by relatively high value of the ε_{GWS} and simultaneously by a low skewness. Preliminary tests presented in [1] show that grasps with low skewness were significantly more robust than grasps with high one, and indicated that humans tend to align their hands with main axes of the grasped object. To compute a deviation of the actual relative pose of the object to the hand from the initial relative pose we adapt a grasp quality score proposed in [12]. This score can be obtained by

$$Q_3 = \begin{cases} 1 - \frac{\delta}{\Delta} & \text{if} \quad \delta < \Delta \\ 0 & \text{if} \quad \delta \geqslant \Delta \end{cases} \tag{11}$$

where δ is the pose deviation, and Δ is a deviation limit which is introduced to normalize the deviation and defined by the user. The deviation in the position and orientation are considered separately and computed as

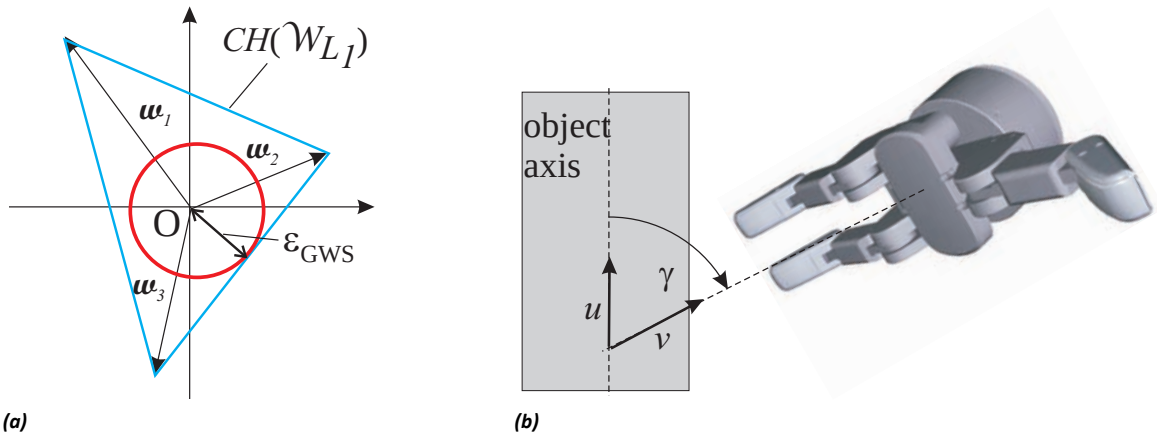

Fig. 5. Illustration of grasp quality measures: (a) a 2D example of ε_{GWS}, (b) relative orientation of the object and robot hand

follows

$$\delta_p = \|\boldsymbol{p}_c - \hat{\boldsymbol{p}}_c\|, \quad \delta_o = \Phi(\hat{q}_c, q_c) = \arccos(|\hat{q}_c \cdot q_c|) \tag{12}$$

where $\boldsymbol{p}_c \in \mathbb{R}^3$ and q_c (a unit quaternion), denote the relative position and orientation of the object coordinate frame with respect to the hand coordinate frame, and the "hat" symbol represents the reference value for measuring the deviation. It should be noted that δ_p and δ_o are invariant under change of coordinate frames for both the hand and the object. Metric $\Phi : \mathbb{S}^1 \times \mathbb{S}^1 \rightarrow \mathbb{R}_+$ is defined as arccos of the inner product of unit quaternions. Since it is essential that Φ is a non-negative function, the angles returned by arccos must be in the first quadrant, i.e., the range of values mapped by Φ is $[0, \pi/2]$. Φ is a pseudometric on the unit quaternions, but a metric on $\mathbb{SO}(3)$.

Stable grasps are defined as those for which all three quality values are within a certain threshold. These thresholds should be determined experimentally.

4. Grasp Synthesis for Known Objects

We assume the existence of a database with 3D models of all the objects encountered in the robot environment, a 3D geometric and kinematic models of the robotic hand executing the grasp. Moreover, we assume that the dynamic model of the grasped object is available. In the proposed approach we use a concept of *grasp preshapes* or *grasp patterns*. Grasp preshape is a hand posture appropriate for the target object and task to be performed.

From a practical point of view, given an object, a grasp can be described by the following characteristics:

- Grasp type – a qualitative description of the grasp to be performed (e.g. a precision or power grasp).
- Hand initial posture – an initial configuration of the fingers.
- Grasp starting pose – a position and orientation of the hand near to the object where the hand is positioned for approaching the object.
- Approach direction – a direction along which the hand approaches the object. All approaching directions are given with respect to an object-centered coordinate system.

To perform a grasp, the hand is positioned and preshaped according to the grasp descriptors and moves along the approaching line. Then the hand is closed by flexing all of the finger joints until contact with the target object stops all motion. A main advantage of this grasp representation is its practical application. Grasp type maybe determined by task specification that describes relations between objects in the environment and action to be performed [24, 28]. This grasp representation is particulary well suited for simple two- or three-fingered robotic hand with fingers having 2 or 3 degrees of freedom, such as the Barrett Hand (Fig. 6). The Barrett hand is an eight-axis, a three-fingered mechanical grasper with each finger having two joints. While one finger (called the thumb) is stationary, the other two fingers can spread synchronously from $0°$ to $180°$ about the palm from the third finger. Each finger has two joints but only the proximal link is actuated. The distal link is coupled to the proximal one and it moves with it at a fixed rate. This hand has in total 4 active degrees of freedom. The first step of the grasp synthesis process is to generate a set of approach directions and grasp starting poses.

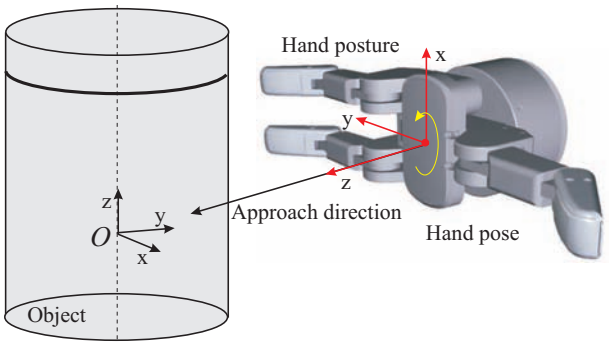

Fig. 6. Grasp description

To perform this task, we use a 3D geometric model of the object defined by the appropriate superquadrics. These models may consist of shape primitives such as spheres, cylinders, cones and boxes or more complex shapes given as a combination of superquadrics. The choice of the shape models will determine the different strategies used to grasp the object. For every given shape we can determine a set of approach directions and grasp starting poses for the hand close to the object. Some approach directions for selected primitive shapes are shown in Figure 7. For each object model

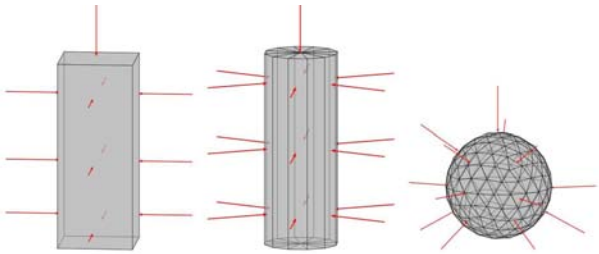

Fig. 7. Selected approach directions for primitive shapes

we compute a set of force closure grasps and previously defined grasps quality measures using a simulator. In each iteration we use the same grasping action, but a different initial pose of the object. The set of poses are chosen to be a discrete approximation of the object's pose uncertainty distribution. The grasp is determined by simulating a grasping heuristic for closing the fingers around the object until contact is made or joint limits are reached. Full 3D rigid body dynamics of the object is considered to compute its motion interacting with the robotic hand and the supporting plane during the grasping process. For simulating object dynamics ODE (Open Dynamics Engine) library is employed [18]. The key advantage of grasp synthesis using such a simulation is the ability to remove grasps that might seem analytically promising but would fail if executed in reality.

5. Conclusions

In this paper, a method for grasp synthesis for a multi-fingered robotic hand under object pose uncertainty based on dynamic simulation was proposed. To model object shape superquadrics was used. To evaluate grasp quality three different measures were utilised. We are convinced that considering both object dynamics and pose uncertainty in the simulation can bring a significant improvement in performance of grasping and manipulation tasks in the real-world environments. The future work will be focused on implementation and testing the proposed grasp synthesis method on the two-arm robot Velma with two Kuka LWR+ arms and Barrett Hands. Visual and tactile sensor will be used to adjust planned grasp during execution.

ACKNOWLEDGEMENTS

The author acknowledges the support of National Centre for Research and Development grant no. PBS1/A3/8/2012.

AUTHOR

Wojciech Szynkiewicz – Institute of Control and Computation Engineering, Warsaw University of Technology, ul. Nowowiejska 15/19, 00–665 Warsaw, Poland, e-mail: W.Szynkiewicz@elka.pw.edu.pl.

REFERENCES

[1] R. Balasubramanian, L. Xu, P. D. Brook, J. R. Smith, and Y. Matsuoka, "Physical human interactive guidance: Identifying grasping principles from human-planned grasps", *IEEE Transactions on Robotics*, vol. 28, no. 4, 2012, 899–910. DOI: 10.1007/978-3-319-03017-3$_2$2.

[2] A. Barr, "Superquadrics and angle-preserving transformations", *IEEE Computer Graphics and Applications*, vol. 1, no. 1, 1981, 11–23.

[3] J. Bohg, A. Morales, T. Asfour, and D. Kragic, "Data-driven grasp synthesis – a survey", *IEEE Transactions on Robotics*, vol. 30, no. 2, 2014, 289–309. DOI: 10.1109/TRO.2013.2289018.

[4] R. Brost, "Automatic grasp planning in the presence of uncertainty". In: *IEEE International Conference on Robotics and Automation (ICRA)*, vol. 3, 1986, 1575–1581. DOI: 10.1109/ROBOT.1986.1087523.

[5] V. N. Christopoulos, P. R. Schrater, "Handling shape and contact location uncertainty in grasping two-dimensional planar objects". In: *Proceedings of International Conference on Intelligent Robots and Systems (IROS)*, 2007, 1557–1563. DOI: 10.1109/IROS.2007.4399509.

[6] H. Dang, P. K. Allen, "Stable grasping under pose uncertainty using tactile feedback", *Autonomous Robots*, vol. 36, no. 4, 2014, 309–330. DOI: 10.1007/s10514-013-9355-y.

[7] R. Diankov *Openrave simulation environmen*t. http://openrave.org/.

[8] C. Ferrari, J. Canny, "Planning optimal grasps". In: *IEEE International Conference on Robotics and Automation*, Nice, France, 1992, 2290–2295. DOI: 10.1109/ROBOT.1992.219918.

[9] I. Gilitschenski, G. Kurz, S. Julier, U. Hanebeck, "A new probability distribution for simultaneous representation of uncertain position and orientation". In: 17^{th} *International Conference on Information Fusion (FUSION)*, 2014.

[10] K. Hsiao, L. P. Kaelbling, T. Lozano-Pérez, "Robust grasping under object pose uncertainty", *Autonomous Robots*, vol. 31, no. 2-3, 2011, 253–268. DOI: 10.1007/s10514-011-9243-2.

[11] A. Kasinski, *Metody syntezy chwytu dla autonomicznych systemów manipulacyjnych* (Grasp

synthesis methods for autonomous manual systems), Poznan Univ. of Tech. Publ. House, 1998, (in Polish).

[12] J. Kim, K. Iwamoto, J. J. Kuffner, Y. Ota, N. S. Pollard, "Physically based grasp quality evaluation under pose uncertainty", *IEEE Transactions on Robotics*, vol. 29, no. 6, 2013, 1423–1439. DOI: 10.1109/TRO.2013.2273846.

[13] T. Kornuta, M. Stefanczyk, W. Kasprzak. "Basic 3D solid recognition in RGB-D images". In: R. Szewczyk, C. Zielinski, M. Kaliczynska, eds., *Recent Advances in Automation, Robotics and Measuring Techniques*, volume 267 of *Advances in Intelligent Systems and Computing (AISC)*, chapter 40, 421–430. Springer, 2014. DOI: 10.1007/978-3-319-05353-0$_4$0.

[14] J. Laaksonen, E. Nikandrova, V. Kyrki, "Probabilistic sensor-based grasping". In: *IIEEE/RSJ International Conference on Intelligent Robots and Systems (IROS)*, 2012, 2019–2026. DOI: 10.1109/IROS.2012.6385621.

[15] Z. Li, S. S. Sastry, "Task-oriented optimal grasping by multifingered robotic hands", *IEEE Journal of Robotics and Automation*, vol. 4, no. 1, 1988, 32–44.

[16] R. M. Murray, Z. Li, and S. S. Sastry, *A Mathematical Introduction to Robotic Manipulation*, CRC Press, 1994. DOI: Task-oriented optimal grasping by multifingered robotic hands.

[17] J. Napier, "The prehensile movements of the human hand", *The Journal of bone and joint surgery*, vol. 38-B, no. 4, 1956, 902–913.

[18] ODE. "Open Dynamics Engine". http://ode.org/.

[19] F. T. Pokorny, D. Kragic, "Classical grasp quality evaluation: New algorithms and theory". In: *IEEE/RSJ International Conference on Intelligent Robots and Systems (IROS)*, 2013. DOI: 10.1109/IROS.2013.6696854.

[20] D. Prattichizzo, J. Trinkle, *Springer Handbook of Robotics*, chapter 28, Springer 2008, 671–700.

[21] S. Sahbani, A. El-Khoury, P. Bidaud, "An overview of 3D object grasp synthesis algorithms", *Robotics and Autonomous Systems*, vol. 60, no. 3, 2012, 326–336. DOI: 10.1016/j.robot.2011.07.016.

[22] K. Shimoga, "Robot grasp synthesis algorithms: A survey", *Int. Journal of Robotics Research*, vol. 15, no. 3, 1906, 230–266. DOi: 10.1177/027836499601500302.

[23] M. Strand, Z. X., M. Zoellner, R. Dillmann, "Using superquadrics for the approximation of objects and its application to grasping". In: *IEEE International Conference on Robotics and Automation (ICRA)*, no. 48–53, 2010. DOI: 10.1109/ICINFA.2010.5512331.

[24] W. Szynkiewicz, "Skill-based bimanual manipulation planning", *Journal of Telecommunications and Information Technology*, no. 4, 2012, 54–62.

[25] J. Weisz, P. K. Allen, "Pose error robust grasping from contact wrench space metrics". In: *IEEE International Conference on Robotics and Automation (ICRA)*, 2012, 557–562. DOi: 10.1109/ICRA.2012.6224697.

[26] O. Williams, A. Fitzgibbon, "Gaussian process implicit surfaces". In: *Gaussian Processes in Practice Workshop*, 2007.

[27] Y. Zheng, "An efficient algorithm for a grasp quality measure", *IEEE Transactions on Robotics*, vol. 29, no. 2, 2013, 579–585. DOI: 10.1109/TRO.2012.2222274.

[28] C. Zielinski, T. Kornuta. "Specification of tasks in terms of object-level relations for a two-handed robot". In: R. Szewczyk, C. Zieli□ski, and M. Kaliczy□ska, eds., *Recent Advances in Automation, Robotics and Measuring Techniques*, volume 267 of *Advances in Intelligent Systems and Computing (AISC)*, 543–552. Springer, 2014. DOI: 10.1007/978-3-319-05353-0$_4$0.